



## Article

# Behaviour of the Blazar CTA 102 during Two Giant Outbursts

Valeri M. Larionov <sup>1,\*</sup> , Svetlana G. Jorstad <sup>1,2</sup> , Alan P. Marscher <sup>2</sup> , Paul S. Smith <sup>3</sup>,  
Sergey Savchenko <sup>1</sup> , Daria Morozova <sup>1</sup> , Tatiana Grishina <sup>1</sup>, Evgenia Kopatskaya <sup>1</sup>,  
Liudmila Larionova <sup>1</sup>, Elena Larionova <sup>1</sup>, Anna Mokrushina <sup>1</sup>, Ivan Troitsky <sup>1</sup>, Yulia Troitskaya <sup>1</sup>  
and George Borman <sup>4</sup>

<sup>1</sup> Astronomical Institute, Saint Petersburg State University, 198504 Saint Petersburg, Russia; jorstad@bu.edu (S.G.J.); savchenko.s.s@gmail.com (S.S.); comitcont@gmail.com (D.M.); azt8@mail.ru (T.G.); enik1346@rambler.ru (E.K.); lliudmila@yandex.ru (L.L.); sung2v@mail.ru (E.L.); hobbitenka1608@rambler.ru (A.M.); dernord@gmail.com (I.T.); yulka19391389@mail.ru (Y.T.)

<sup>2</sup> Institute for Astrophysical Research, Boston University, Boston, MA 02215, USA; marscher@bu.edu

<sup>3</sup> Steward Observatory, University of Arizona, Tucson, AZ 85721, USA; psmith@as.arizona.edu

<sup>4</sup> Crimean Astrophysical Observatory, Nauchny, Crimea 298409, Russia; borman.ga@gmail.com

\* Correspondence: v.larionov@spbu.ru

Received: 23 September 2017; Accepted: 27 November 2017; Published: 30 November 2017

**Abstract:** Blazar CTA 102 underwent exceptional optical and high-energy outbursts in 2012 and 2016–2017. We analyze its behaviour during these events, focusing on polarimetry as a tool that allows us to trace changes in the physical conditions and geometric configuration of the emission source close to the central black hole. We also use *Fermi*  $\gamma$ -ray data in conjunction with optical photometry in an effort to localize the origin of the outbursts.

**Keywords:** blazars; photometry; polarimetry; methods of analysis

## 1. Introduction

The importance of monitoring projects in blazar studies was clear from the discovery of these objects due to their violent variability on time scales from minutes to years. Outbursts that may occur unexpectedly for any given source, act like a magnifying glass that allow us to penetrate deeper into the most suspicious regions of the inner jet. Numerous successful campaigns were carried out that lead to a systematic accumulation of observational data, either involving a single observatory or large international collaborations. Particularly, the massive Whole Earth Blazar Telescope (WEBT) campaign was undertaken during a huge CTA 102 outburst [1]. The main findings of this campaign are the co-spatiality of the synchrotron and inverse Compton emission sites and the detection of a clockwise rotation of the polarization vector during the maximum of the outburst. It was shown that both the photometric and polarimetric behaviour of CTA 102 agrees with the model of a helical jet whose axis became closer to our line of sight beginning in 2012. The decrease of the viewing angle of the CTA 102 jet is also supported by VLBA observations [2]. Correspondingly, one could expect that flaring activity in this blazar will remain pronounced as long as the jet viewing angle remains small.

This prediction proved to be true at the end of 2016, when CTA 102 entered a new phase of high activity that culminated in a huge outburst that far surpassed all previous recorded flares for this blazar. In this paper we report preliminary results of our photometric and polarimetric observations of CTA 102 during this unprecedented event. A more detailed analysis awaits a dedicated WEBT paper. In Section 2.1 we describe our optical data analysis. Section 2.2 reports the results of  $\gamma$ -ray data, in Section 3 we discuss our findings and in Section 4 summarize the results.

## 2. Observations

### 2.1. Optical Data

We use optical photometric and polarimetric *R*-band data collected at St. Petersburg University (Crimea and St. Petersburg), see [3], Lowell (Perkins) [4] and Steward observatories [5]. We also use data from [1] for comparison. When analysing the position angle variability, we resolve the  $\pm 180^\circ$  ambiguity by adding/subtracting  $180^\circ$  each time that the subsequent value of the electric vector position angle (EVPA) is  $>90^\circ$  less/more than the preceding one (see [1]).

### 2.2. $\gamma$ -Ray Data

To process  $\gamma$ -ray data we use the standard Fermi analysis software package Science Tools v10r0p5<sup>1</sup>, with the instrument response function P8R2\_V6, the Galactic diffuse emission model gll\_iem\_v06, and the isotropic background model iso\_P8R2\_SOURCE\_V6\_v06.

Our background model includes all sources from the 3FGL catalog within  $15^\circ$  of CTA 102. For all background sources within  $10^\circ$ , fluxes were set as a free parameter, whereas fluxes of sources beyond  $10^\circ$  were fixed to their 3FGL four-year mean values. CTA 102 itself was modelled as a point source with a log-parabolic spectrum having spectral parameters fixed to its catalog values.

In order to obtain the highest possible temporal resolution of the  $\gamma$ -ray light curve, we adaptively bin the observed time range. The main idea is to split the entire time range into bins of variable lengths such that periods of active states (high flux) have finer binning than during quiet states (low flux). We use the Test Statistic (TS) value to estimate the significance of the  $\gamma$ -ray signal. The square root of the TS value roughly corresponds to the significance of the source detection. The following algorithm is used to set the bin size. We start with 0.25 day bins and gradually increase their size until we obtain  $TS = 100$ . If we reach one-week-long bins, but the TS value is still under 100, we change the desired value of TS to 10 to prevent the creation of bins that are too wide. Usually, the trade off between detection significance and bin size leads to the creation of one-week-long bins with  $10 < TS < 100$ . During rare periods of very low  $\gamma$ -ray flux, even one-week bins are not enough to achieve  $TS = 10$  and we increase the integration time to more than one week. If we reach a 30-day-long bin, but still have  $TS < 10$ , we use an upper limit flux estimation for that time period and then start a new bin.

This algorithm of the adaptive binning could be less computationally efficient for some objects than the one described in [6], since for every bin size search, we need to repeatedly perform all the analysis until the optimal length is found. On the other hand, our approach is more straightforward since it performs all the standard likelihood pipeline without shortcuts and does not impose any assumptions (such as monotonic increase of the TS value with the integration time).

The results of our optical photometric and polarimetric monitoring of CTA 102, together with  $\gamma$ -ray data, are shown in Figure 1.

---

<sup>1</sup> <https://fermi.gsfc.nasa.gov/ssc/data/analysis/software/>

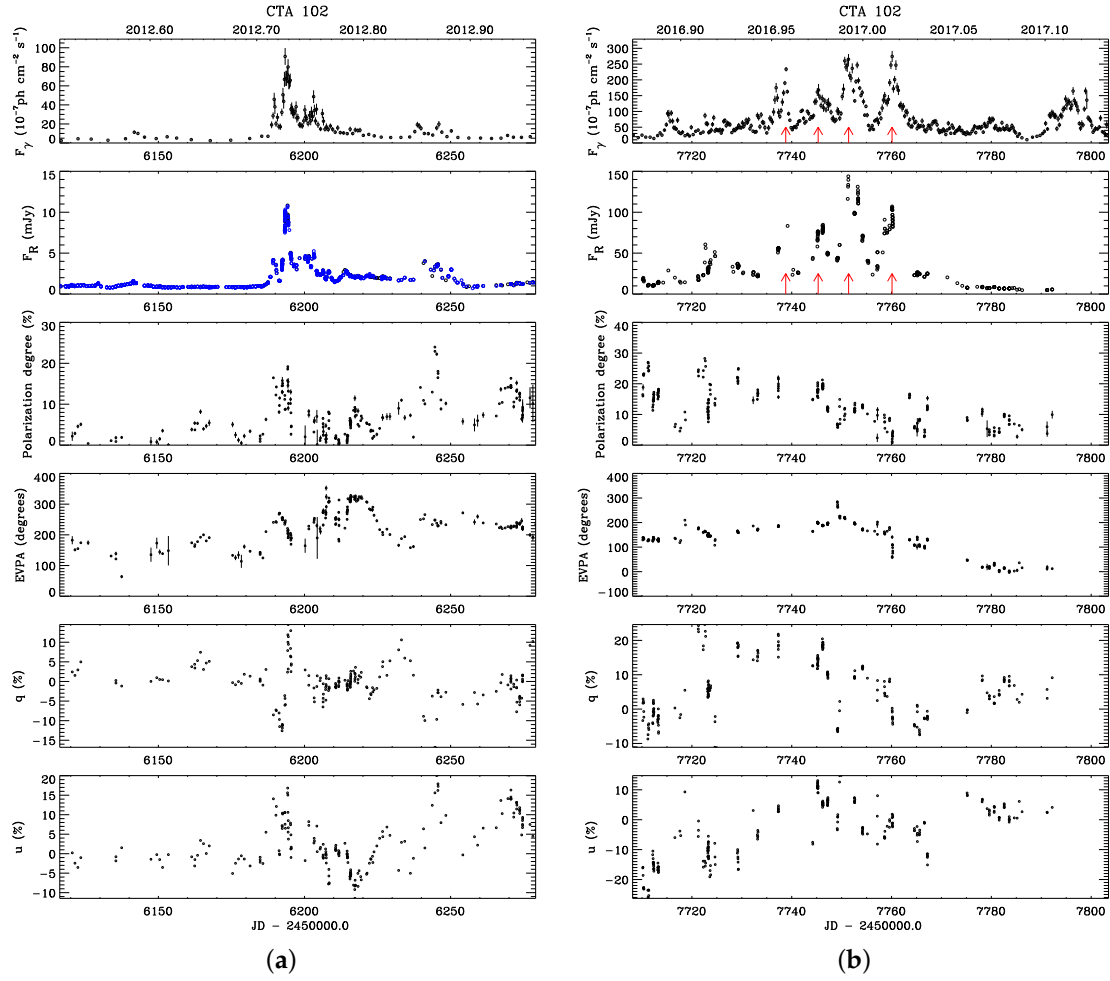


**Figure 1.** (a) From top to bottom:  $\gamma$ -ray flux evolution; optical R-band flux evolution, optical fractional polarization, position angle of polarization, and normalized Stokes parameters for CTA 102 during the outburst of 2012, adapted from [1]; (b) The same for the outburst of 2016–2017. Red arrows mark positions of four subflares. Notice the different time and flux scales for the two observing seasons.

### 3. Results and Discussion

#### 3.1. Optical – $\gamma$ -Ray Correlations

A traditional approach to test whether optical and  $\gamma$ -ray radiation arise in the same part of blazar's jet is to use the Discrete Correlation Function, DCF, as suggested in [7]. We calculated DCFs separately for the 2012 and 2016–2017 CTA 102 outbursts. These results are presented in Figure 2. In order to determine the DCF peak position uncertainty, we utilized a bootstrap + flux randomization Monte Carlo simulation [8]. The results based on 1000 runs are  $\tau = 0.73 \pm 0.50$  days for the event of 2012 and  $\tau = 0.54 \pm 1.03$  days for the event of 2016–2017.

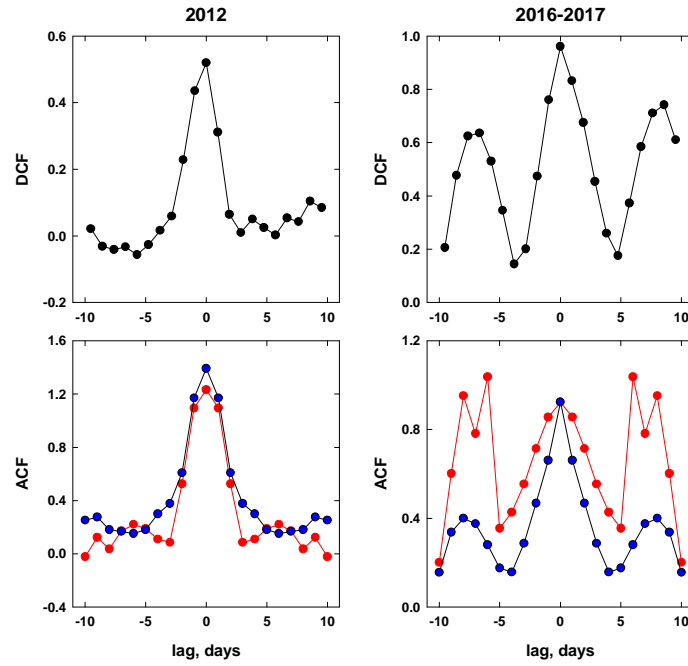


**Figure 2.** **Upper left:** Discrete Correlation Function (DCF) of optical R-band flux and  $\gamma$ -ray flux for CTA 102 during the outburst of 2012, adapted from [1]. **Upper right:** The same for the outburst of 2016–2017. **Bottom panel:** auto-correlation functions for corresponding time intervals: red—for optical R flux, blue—for  $\gamma$ -ray flux. During both outbursts, there are no delays between  $\gamma$ -rays and optical, implying that the sites of synchrotron and IC radiation are co-spatial. The triple DCF in 2016–2017 is a consequence of  $\sim 7$  days recurrence of optical and  $\gamma$ -ray outbursts (see also Figure 1b).

As is evident from Figure 2, there is no delay between changes of fluxes in the synchrotron and inverse Compton (IC) parts of the CTA 102 spectrum. This implies that the sites of synchrotron and IC radiation are co-spatial. The triple-peaked DCF in 2016–2017 is a consequence of the  $\sim 7$  days recurrence of optical and  $\gamma$ -ray outbursts (see Figure 1b and auto-correlation plots in Figure 2). This lack of delay allows us to compare directly the optical and  $\gamma$ -ray flux densities. To do this, we (1) bin the R-band optical data so that the mid-point and size of each optical bin corresponds to the mid-point and size of the respective  $\gamma$ -ray bin, and (2) subtract from the binned optical data a tentative value 0.45 mJy of the flux of (quasi-)permanent emission components, as suggested in [1]. In Figure 3 we show the optical and  $\gamma$ -ray flux evolution from 2008 to 2017. Figure 4 reveals dramatic differences during various stages of CTA 102 activity. These stages are colour-encoded in the way shown in Figure 3. One may immediately notice that slopes during ‘silent’ time intervals (blue, pink and green circles) are close to 2. In contrast, during moderately high activity (red and black) the slope is close to 1. The slope of 2 may correspond to synchrotron self-Compton (SSC) as a dominant source of IC radiation. A slope of unity is better explained as a result of changed viewing angle, leading to the changes in Doppler factor, as suggested in [1]. The exceptional outburst of 2016–2017 also follows a slope of unity, but substantially displaced (0.6 dex downward, which corresponds to  $\approx 4$  times lower  $\gamma$ -ray flux. This may reflect, as suggested in [9], a decreased Compton dominance for the radiating region that may be located substantially farther downstream from the central BH than the region responsible for the 2012 outburst. Alternatively, the seed photon field at a given distance from the central engine could be time-variable, as then would be the inverse Compton flux at that location.

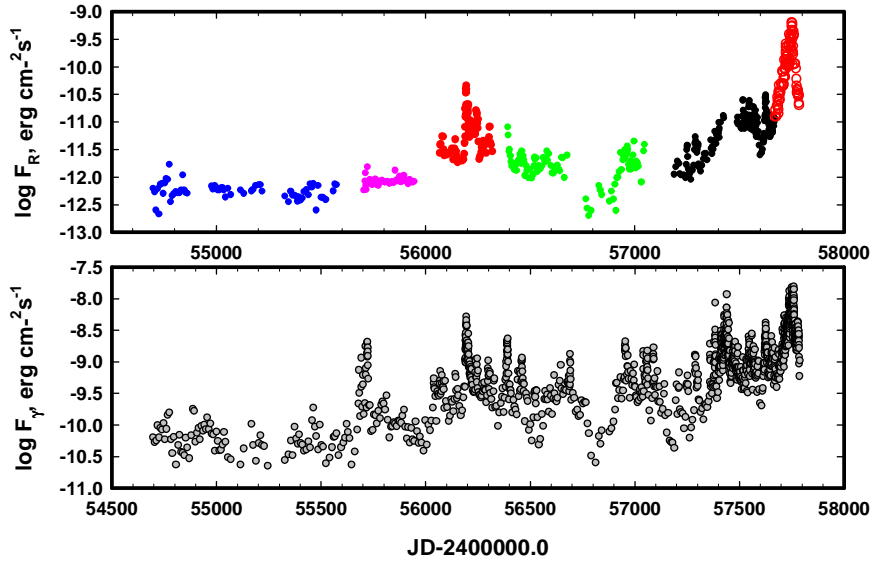


**Figure 3.** Optical and  $\gamma$ -ray flux evolution from 2008 to 2017 with colour encoded in the upper optical panel corresponding to different stages of activity.

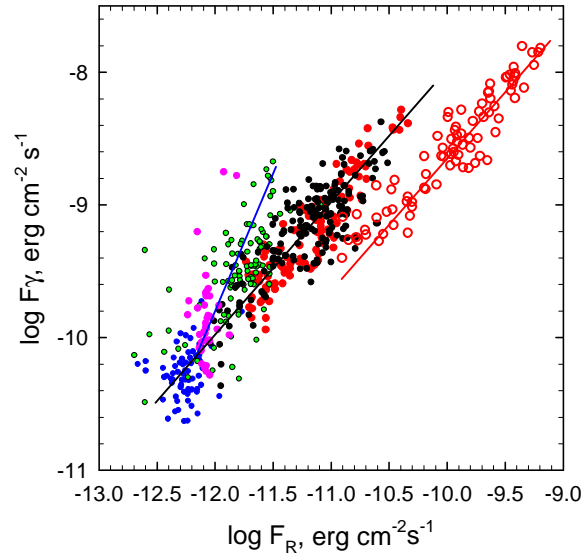


**Figure 4.** Optical –  $\gamma$ -ray flux-flux diagram. Slopes during ‘silent’ time intervals (blue, pink and green circles) are close to 2. A slope close to 1 is observed during periods of higher activity. The exceptional outburst of 2016–2017 (red open circles) also follows a slope of unity, but is substantially (0.6 dex) displaced from the measurements of the previous epochs.

### 3.2. Polarimetric Behaviour

CTA 102 is a typical blazar in the sense that it possesses strong and highly variable polarization. As noted in [1], both the amount and dispersion of the degree of polarization substantially increased with the onset of CTA 102 activity in 2012. The positive correlation between flux and polarization degree (PD) during the 2012 outburst is naturally explained within a model of a moving blob or shock wave and decreased viewing angle. The same model may be applied to explain the flux – PD dependence observed in 2016–2017. In Figure 5 (left panel) green circles correspond to 2012 data and black circles to the 2016–2017 data. If the general shape of the variability pattern is explained by the changes in viewing angle, which in 2016–2017 is presumably even smaller than in 2012 (from  $\approx 3^\circ$ ,

see [1], to almost  $0^\circ$ ), then the highest values of Doppler-boosted flux must correspond to the lowest values of PD. The relevant formulas, connecting values of polarization degree, as well as the Lorentz and Doppler factors, with the viewing angle, plasma compression ratio and the slope of synchrotron spectrum may be found, e.g., in [10]. Models with Lorentz factor  $\Gamma = 37$ , spectral index of synchrotron spectrum  $\alpha = 1.1$ , and plasma compression ratio  $\eta = 1.5$  and  $\eta = 1.3$  are shown by the blue and red curves, respectively.

The right panel of the same figure gives the distribution of the position angles of the optical polarization (EVPA) during both outbursts. The substantial displacement of the two distributions relative to each other,  $\sim 60^\circ$ , suggests a large transverse shift of radiating sites between the two outbursts. This provides an additional evidence of a difference in the 3D location of the 2012 and 2016–2017 outbursts (1) along the jet; (2) in viewing angle and (3) in position angle.

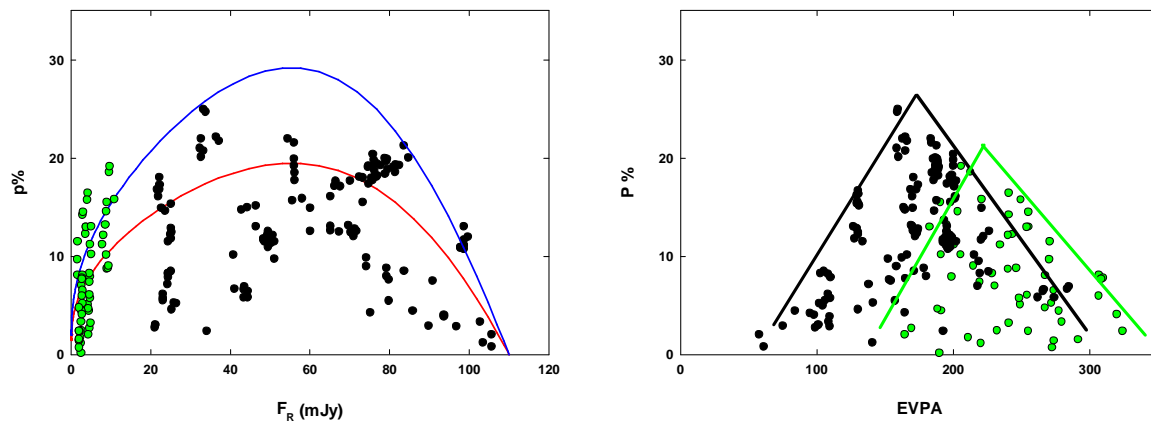


**Figure 5.** **Left:** Dependence of CTA 102 optical polarization on  $R$ -band flux density. Green circles correspond to the 2012 outburst and black to the outburst of 2016–2017. Curves correspond to expectations of a model that explains most flux and polarization variations with changing viewing angle. The red curve corresponds to a plasma compression ratio of  $\eta = 1.3$ . The blue curve has  $\eta = 1.5$ . **Right:** Dependence of optical polarization on EVPA for 2012 (green) and 2016–2017 (black).

#### 4. Conclusions

The results of our analysis of optical photometry and polarimetry of CTA 102 obtained during its outburst of 2016–2017, in conjunction with the analysis of *Fermi*  $\gamma$ -ray data, may be briefly summarized as follows:

- During both outbursts there are no delays between  $\gamma$ -rays and optical flux variations. This means that the sites of synchrotron and IC radiation are co-spatial.
- The dependence of the degree of polarization vs. flux density in  $R$  band during the 2016–2017 outburst reflects both a smaller viewing angle and a higher Lorentz-factor than during 2012 event.
- The shift of the  $\log F_{opt}$  vs  $\log F_\gamma$  dependence may be caused by the location of the 2016–2017 outburst being substantially farther downstream from the BH than during the 2012 event. A location of the 2016 outburst farther from the BH than the 2012 outburst is supported by the fact that its Lorentz factor is substantially higher ( $\Gamma = 37$ ) than during the 2012 outburst ( $\Gamma = 18.2$ , [1],  $\Gamma_{var} = 17.3$ , [2]).

**Acknowledgments:** The St.Petersburg University team acknowledges support from Russian Science Foundation grant 17-12-01029. V.L. acknowledges support from St.-Petersburg University travel grant 6.41.340.2017. The BU group acknowledges support from National Science Foundation grant AST-1615796. Blazar research at Steward Observatory is supported by NASA/*Fermi* Guest Investigator grant NNX15AU81G.

**Author Contributions:** All authors have participated in both the analysis and the scientific discussion.

**Conflicts of Interest:** The authors declare no conflict of interest.

## References

1. Larionov, V.M.; Villata, M.; Raiteri, C.M.; Jorstad, S.G.; Marscher, A.P.; Agudo, I.; Smith, P.S.; Acosta-Pulido, J.A.; Arévalo, M.J.; Arkharov, A.A.; et al. Exceptional outburst of the blazar CTA 102 in 2012: The GASP-WEBT campaign and its extension. *Mon. Not. R. Astron. Soc.* **2016**, *461*, 3047, doi:10.1093/mnras/stw1516.
2. Casadio, C.; Gómez, J.L.; Jorstad, S.G.; Marscher, A.P.; Larionov, V.M.; Smith, P.S.; Gurwell, M.A.; Lähteenmäki, A.; Agudo, I.; Molina, S.N.; et al. A Multi-wavelength Polarimetric Study of the Blazar CTA 102 during a Gamma-Ray Flare in 2012. *Astrophys. J.* **2015**, *813*, 51, doi:10.1088/0004-637X/813/1/51.
3. Larionov, V.M.; Jorstad, S.G.; Marscher, A.P.; Raiteri, C.M.; Villata, M.; Agudo, I.; Aller, M.F.; Arkharov, A.A.; Asfandiyarov, I.M.; Bach, U.; et al. Results of WEBT, VLBA and RXTE monitoring of 3C 279 during 2006–2007. *Astron. Astrophys.* **2008**, *492*, 389–400, doi:10.1051/0004-6361:200810937.
4. Jorstad, S.G.; Marscher, A.P.; Larionov, V.M.; Agudo, I.; Smith, P.S.; Gurwell, M.; Lähteenmäki, A.; Tornikoski, M.; Markowitz, A.; Arkharov, A.A.; et al. Flaring Behavior of the Quasar 3C 454.3 Across the Electromagnetic Spectrum. *Astrophys. J.* **2010**, *715*, 362, doi:10.1088/0004-637X/715/1/362.
5. Smith, P.S.; Montiel, E.; Rightley, S.; Turner, J.; Schmidt, G.D.; Jannuzi, B.T. Coordinated Fermi/Optical Monitoring of Blazars and the Great 2009 September Gamma-ray Flare of 3C 454.3. *arXiv* **2009**, arXiv:0912.3621.
6. Lott, B.; Escande, L.; Larsson, S.; Ballet, J. An adaptive-binning method for generating constant-uncertainty/constant-significance light curves with Fermi-LAT data. *Astron. Astrophys.* **2012**, *544*, A6, doi:10.1051/0004-6361/201218873.
7. Edelson, R.A.; Krolik, J.H. The discrete correlation function—A new method for analyzing unevenly sampled variability data. *Astrophys. J.* **1988**, *333*, 646–659.
8. Peterson, B.M.; Wanders, I.; Horne, K.; Collier, S.; Alexander, T.; Kaspi, S.; Maoz, D. On Uncertainties in Cross-Correlation Lags and the Reality of Wavelength-dependent Continuum Lags in Active Galactic Nuclei. *Publ. Astron. Soc. Pac.* **1998**, *110*, 660–670.
9. Ghisellini, G.; Tavecchio, F. Canonical high-power blazars. *Mon. Not. R. Astron. Soc.* **2009**, *397*, 985, doi:10.1111/j.1365-2966.2009.15007.x.
10. Larionov, V.M.; Jorstad, S.G.; Marscher, A.P.; Morozova, D.A.; Blinov, D.A.; Hagen-Thorn, V.A.; Konstantinova, T.S.; Kopatskaya, E.N.; Larionova, L.V.; Larionova, E.G.; et al. The Outburst of the Blazar S5 0716+71 in 2011 October: Shock in a Helical Jet. *Astrophys. J.* **2013**, *768*, 40, doi:10.1088/0004-637X/768/1/40.



© 2017 by the authors. Licensee MDPI, Basel, Switzerland. This article is an open access article distributed under the terms and conditions of the Creative Commons Attribution (CC BY) license (<http://creativecommons.org/licenses/by/4.0/>).